Laser-induced choroidal neovascularization model in mice

Vincent Lambert[1, 2], Julie Lecomte[2], Sylvain Hansen[2], Silvia Blacher[2], Maria-Luz Alvarez Gonzalez[2], Ingrid Struman[3], Nor Eddine Sounni[2], Eric Rozet[4], Pascal de Tullio[5], Jean Michel Foidart[2], Jean-Marie Rakic[1], Agnès Noel[2]

[1]Department of Ophthalmology, University Hospital (CHU), Liège, Belgium. [2]Laboratory of Tumor and Development Biology, GIGA-Cancer, University of Liège, Liège, Belgium. [3]Unit of Molecular Biology and Genetic Engineering, GIGA-Cancer, University of Liège, Liège, Belgium. [4]Analytical Chemistry Laboratory (CIRM), University of Liège, Liège, Belgium. [5]Drug Research Center (CIRM), University of Liège, Liège, Belgium.

Correspondence should be addressed to A.N. (agnes.noel@ulg.ac.be; phone: +32-43662569; fax: +32-43662936)

ABSTRACT

The mouse model of laser-induced choroidal neovascularization (CNV) has been used extensively in studies of the exudative form of age-related macular degeneration (AMD). This experimental *in vivo* model relies on laser injury to perforate Bruch's membrane, resulting in sub-retinal blood vessel recruitment from the choroid. By recapitulating the main features of the exudative form of human AMD, this assay has served as the backbone for testing anti-angiogenic therapies. This standardized protocol can be applied to transgenic mice and can include treatments with drugs, recombinant proteins, antibodies, adenovirus and pre-miR to aid in the search for new molecular regulators and the identification of novel targets for innovative treatments. This robust assay requires 7-14 days to complete, depending on the treatment applied and whether immunostaining is performed. This protocol includes details of

how to induce CNV, including laser induction, lesion excision, processing plus different approaches to quantify neoformed vasculature.

INTRODUCTION

Age-related macular degeneration (AMD) is the leading cause of vision loss in Europe, the USA and Australia [1]. Almost two-thirds of the population over 80 years old will have signs of AMD [2-4] resulting from the wet or exudative form, which is characterized by the presence of drusen and choroidal neovascularization (CNV). The first studies performed on CNV associated with AMD aimed to compare mRNA and protein levels in human neovascular membranes excised surgically *versus* intact choroids. Experimental animal models rapidly became essential for elucidating the cellular and molecular mechanisms involved in CNV pathogenesis and for the screening of new drugs. Indeed, no *in vitro* model developed to date recapitulates the complex CNV-associated processes that involve, at a minimum, several cell types, such as inflammatory cells, endothelial cells, pericytes, bone marrow (BM)-derived cells, myofibroblasts and glial cells [5, 6]. The *in vivo* exploration of CNV currently involves several murine models exhibiting the spontaneous development of CNV resulting from a defective complement-activating pathway, deletion in a chemokine/chemokine receptor, oxidative damage or aging [7]. Currently, the laser-induced Bruch's membrane photocoagulation model is the most widely accepted and most frequently utilized experimental murine CNV model. The model described here consists of the laser impact rupturing of Bruch's membrane, which leads to the growth of new blood vessels from the choroid into the sub-retinal space, mimicking the main characteristics of the exudative form of human AMD [8] and offering the opportunity to explore the molecular mechanism of CNV through the use of a large panel of transgenic mice. The model has proven to be suitable for testing the efficacy of new drugs through systemic or local (intraocular) administration and

has shown predictive value for drug effects in patients with AMD, for example with VEGFR-trap [9, 10] or anecortave acetate [11, 12]. This model is also appropriate for identifying new potential targets using siRNA/miRNA technology [13].

Development of the CNV assay

The Campochiaro group was the first to induce CNV through laser injury of Bruch's membrane in mice [8]. In this model, inflammatory cells are thought to be potent initiators of the angiogenic process partly through their capacity to release a series of pro-angiogenic factors [6]. Both neutrophil and macrophage depletion reduce CNV formation [14-16]. The recruitment of BM-derived cells (endothelial progenitor cells, pericytes, mesenchymal stem cells) in CNV lesions has been reported [5, 17-19] and mimics the vasculogenic process observed in human patients [17]. Vascular endothelial growth factor (VEGF-A) rapidly emerged as a potent angiogenic factor involved in CNV formation, diverting much of the focus of research. This intensive research led to strategies aimed towards blocking VEGF or its receptors that have been approved by the US Food and Drug Administration (FDA) for AMD treatment [20-22]. This achievement, based on the use of the laser-induced CNV assay, has validated angiogenesis as an important target for AMD treatment [6]. Transgenic mouse technologies have since allowed rapid expansion in the exploration of key regulators of CNV, leading to the identification of other important VEGF family members, such as placental growth factor (PlGF) [23, 24] and proteases [19, 25-28]. More recently, the interplay between complement factor H, the complement membrane attack complex, a chemokine (CCL2) and VEGF during CNV development has been established [29, 30].

Applications of the CNV assay

The CNV assay is a robust, relevant model that mimics AMD disease, with clear advantages over other recently reviewed *in vivo* models [7]. The assay recapitulates the complex biological processes involved in the exudative form of AMD disease (inflammation and angiogenesis) and is relatively rapid to develop on an easily accessible biological tissue that can be flat-mounted or prepared for histological sectioning or on protein or nucleic acid extractions. Furthermore, in contrast to the transgenic models that overexpress apolipoprotein E [31] or with a superoxide dismutase 1 (SOD1) deletion [32], which are long-term assays requiring senescent animals, the laser-induced CNV assay can be applied to a panel of young wild-type or transgenic mice. The model is applicable to transgenic (knock-out or knock-in) mice. In addition, viruses, cells or compounds, including neutralizing antibodies, si/shRNA, pre-miR, recombinant proteins, nanoparticles and drugs, can be administered via different pathways (intraperitoneal injection, intravenous injection, *per os*, drinking water, intravitreous injection, subretinal injection, BM engraftment and others) and combined or not with genetic manipulation [9, 33-37].

Limitations of the CNV assay

In addition to the absence of a defined macula in mice, the rodent laser trauma model is obviously unable to mimic the complexity of human pathology [4]. This model is generated with a wound-healing reaction that follows an insult at the level of Bruch's membrane and relies heavily on inflammation [38, 39]; in contrast, in AMD, genetic susceptibility plays a major role [40]. Factors important for the generation of the model may or may not occur in patients with exudative AMD. The involvement of VEGF [41] and placental growth factor [24] in the progression of experimental CNV has led to the clinical development of specific antagonists, such as ranibizumab [21] and aflibercept (VEGF trap-eye) [10]. Key features of AMD, such as sub-retinal pigmented epithelium (RPE) deposits (drusen) and the influence of age, are either

absent or not crucial in this experimental model. Limitations of the assay also include the requirement of pigmented mice (BL6 mice are preferred) for laser reaction, the necessity of a trauma to induce CNV (no spontaneous development) and spontaneous regression (after 14-21 days). This model is suitable to study exudative AMD but not the atrophic form of this ocular disorder. An important drawback of the model is that it cannot be used to test primate-specific reagents. To overcome this limitation, it is sometimes possible to use mice expressing the human homolog of the protein of interest. For example, to test human-specific VEGF antagonists, a transgenic mouse strain that expresses human VEGF in photoreceptors has been used as an alternative [42].

Overview of the procedure

The general protocol for CNV induction involves laser burning of Bruch's membrane following mouse anesthesia and pupil dilatation, eye resection at defined time point(s), imaging and quantification of angiogenesis and/or inflammation (**Fig. 1**). After anesthesia and pupil dilatation, a laser burn is first induced using a green Argon laser focused on the RPE. The presence of a bubble confirms the success of the laser impact. Mice are housed in the animal facility during the indicated time periods. During this period, treatments can be applied to the mice. After sacrifice, the eyes are resected, and the choroid is either flat-mounted for immunohistological staining, embedded in paraffin or frozen or used for protein or nucleic acid extraction. Blood sample analysis can also be performed, such as for metabolomics studies (**Fig. 1**).

Experimental design

Experimental animals. This protocol is applicable to mice older than 2 weeks when the eyes are open and can be used to evaluate the effects of exogenous agents and/or genetic knock-in

or knock-out. Adult C57BL/6J mice 6-8 weeks old weighing 18-20 g are the most appropriate for the assay, although the model can be applied to other mouse backgrounds provided they have pigmented eyes. It is worth noting that aged mice exhibit more severe CNV [43]. The sex of the mice does not appear to influence the assay substantially, except for older female mice, which develop more severe CNV than do males [44]. Laser burns are induced typically at the 3, 6, 9 and 12 o'clock positions around the optic disc in compliance with national and local ethical committees (Supplemental video 1).

All mice must be treated in accordance with the ARVO Statement for the Use of Animals in Ophthalmic and Vision Research (www.arvo.org). Anesthesia and euthanasia must be performed in accordance with the local animal use committee. The use of ketamine and xylazine mixtures is not recommended because it can lead to serious side effects. At high anesthetic doses, an acute and reversible cataract can occur, leading to lens clouding, which can reduce the visibility of the eye fundus and disturb laser focusing [45].

Because of the inherent variability in animal experiments and because some laser impacts do not result in CNV (approximately 70% of impacts are successful), it has proven necessary to use at least 6 animals, with 4 impacts per eye per experimental group, and to repeat experiments at least twice. Two types of control groups are recommended. The first control group is not subjected to laser induction when comparing transgenic mice and/or evaluating proteins or RNAs or performing metabolomics studies. The second control group consists of mice subjected to laser burns and injected with the vehicle buffer alone for drug efficiency testing. When evaluating pre-miR or siRNA, appropriate scramble sequences are recommended as controls. In cases of BM engraftment, an experimental group consisting of irradiated and BM-engrafted animals is mandatory because we have observed that BM engraftment can impact CNV formation [5, 19]. In general, the use of one eye for drug testing and the second eye as a control is useful because it controls for variation between mice.

However, systemic dissemination of the drug is likely to occur. For example, intraocular injections of bevacizumab suppress subretinal neovascularization in the injected eye and also cause significant suppression in the fellow eye, indicating a systemic effect. In contrast, this is not the case for intraocular injections of ranibizumab [42]. Therefore, investigators should rule out systemic effects in the fellow eye with the drug being tested.

Statistical analysis. To compare the effects of different treatments or compounds (*I)*, including the control groups, on the chosen response, a linear mixed model has to be constructed that corresponds to the experimental setup. The following model can be used:

$$y_{ijkl} = \mu + \tau_i + A_j + B_{k(j)} + \varepsilon_{ijkl}$$

where y_{ijkl} is the response measured (CNV surface); τ_i denotes the fixed effect of the treatments i=1,..,I (staining background, drugs); A_j is the random effect due to animal variability (j=1,…,6) (individual mouse variability); $B_{k(j)}$ is the random effect of the eyes (k=1,2) nested into the animal factor (right or left eye) and ε_{ijkl} represents the residual random error (l=1,…,4 impacts). The statistical significance of the treatment factor τ_i of the model is assessed by comparing its p-value to the significance level e.g. $\alpha = 0.05$. If found significant (p-value<α), adequate post-hoc comparisons of each treatment versus the control group or adequate linear contrasts can be performed to found the promising treatments. We recommend to use a hierarchical mixed Anova for 3 factors. It is worth noting that depending on the nature of the response, a generalized linear mixed model could be used to analyze the data in place of linear mixed model that assumes a normal distribution of the response y_{ijkl}.

Treatment procedure. Intravitreal injection can be performed during anesthesia just after laser induction. Eyes are locally anesthetized, and a first hole is made under the limbus with a 30G needle. The eye is gently massaged with a cotton swab to remove a portion of the vitreous to avoid a post-injection reflux of vitreous and/or drug solution. Then, 2 µl of drug solution in PBS is intravitreously injected through the initial hole using a 34G Hamilton

syringe. Animals injected with PBS alone are used as controls. An alternative procedure consists of direct injection using pulled glass micropipettes attached to a Harvard pump[46]. The latter is easier and less traumatic but may induce some drug solution reflux.

For testing compounds, recombinant proteins [27] or drugs [25] can be administered through single or multiple intraperitoneal (i.p.) injections in a 200-µl solution volume. Standard vehicle-alone treatments should be included for comparison. When evaluating neutralizing antibodies [23, 24], appropriate control antibodies should be used. Recombinant adenovirus (e.g., $7X10^8$ PFU) can be intravenously (i.v.) injected. According to regulatory constraints, virally infected animals are permanently housed under BL2 containment, and sample analyses must be conducted in compliance with governmental and institutional rules.

The involvement of BM-derived cells is demonstrated in BM transplantation experiments [5, 19, 47-50]. BM transplantation experiments involve the isolation of BM cells from the tibias and femurs of donor mice between 8 and 12 weeks of age. Here, BM cells from transgenic mice expressing enhanced green fluorescent protein (GFP) under the control of the β-actin promoter, C57BL/6-Tg(ACTbEGFP)10sb, are collected and grafted into previously irradiated recipient C57BL/6J mice. Total body lethal irradiation is performed and varies from 8-12 Gy for immunocompetent mice. Because of variation in the acute lethal response to whole-body irradiation depending on mouse strain and age, the investigators must define the lethal dose of irradiation. At least 5 weeks are necessary for the mice to recover after BM transplantation. Percentage chimerism can be measured using antibodies against donor-specific cell surface proteins via flow cytometry analysis of blood and BM cells. For GFP+ BM-derived cell transplantation, the percentages of GFP+ donor cells in blood and BM samples are determined by flow cytometry [5, 19].

Sample excision and processing. To visualize the neoformed vascular network, FITC-dextran can be intravenously injected 3 min before mouse sacrifice. Both eyes are resected,

briefly cleaned and prepared for histological analysis, frozen for RNA or protein extraction or fixed in 1% paraformaldehyde for flat-mount analysis. For the latter, eyes are cleaned more precisely after fixation. The excess muscle and optic nerve are removed (Supplemental video 2). The cornea is dissected and removed. The retina is carefully separated from the choroid, and 4 cuts are made to easily flatten the choroid onto the slide (Supplemental video 3). For immunohistochemical analyses of eye sections, we have noted that the blue and brown chromogenic substrates frequently used on paraffin sections are difficult to distinguish from the melanin of RPE and choroid. Therefore, we prefer to use eye cryosections for fluorescent immunostaining. At the end of the assay, blood samples can also be collected for further analyses, such as enzyme-linked immunosorbent assay (ELISA) and metabolomics studies.

Imaging and Quantification. Quantification can be performed on either tissue sections or flat-mounted choroids. Quantitative morphometric assessment of neovascular lesion thickness in eye sections is performed using a computer-assisted image analysis system. Microscopic images (working magnification of 200X) of hematoxylin-stained eye sections are acquired via a video camera, digitized and measured using ImageJ software. Frozen serial sections are cut throughout the extent of each burn, and the thickest lesions (at least 5 sections per lesion) are used for quantitation. Neovascularization is estimated by the ratio (B/C) of lesion thickness from the bottom of the pigmented choroidal layer to the top of the neovascular membrane (B) to the thickness of the intact pigmented choroid adjacent to the lesion (C) (**Fig. 2a**). Histological immunostaining with anti-PECAM and anti-collagen IV antibodies assess the presence of newly formed blood vessels (**Fig. 2b**). The advantage of this quantification method (over surface estimation) is that the B/C ratio is independent of the oblique section (**Fig. 2c**), whereas section orientation influences the measurement of a lesion's surface.

However, this method is time-consuming and requires an entire eye to obtain sufficient sections through all impacts for objective quantification.

We routinely use FITC-dextran-labeled flat-mounted choroid for rapid quantification of neoformed vessels (**Fig. 2d**). For two-dimensional (2D) analysis, images obtained by fluorescence microscopy are digitized using a three-color video camera. ImageJ is used to measure the total area (in μm^2) of CNV associated with each burn. A calibration image is taken from a slide with a grating of known size. An established and constant threshold in pixels (corresponding to threshold fluorescence) is used to quantify neovascularization. The optimum time point to assess CNV formation is typically at day 7 or day 14 (**Fig. 3**). Later, an active healing process begins, and the lesion size decreases.

For three-dimensional (3D) analysis of FITC-dextran-labeled microvessels, images are binarized using the same threshold for all images, and the area of neovascularization is quantified. The spatial distribution of fluorescence is examined using an inverted confocal laser microscope. After 3D fluorescent image construction, the CNV volume is determined using the image analysis toolbox of MATLAB 7.9.

Immunofluorescence staining is required to obtain more information on microvessels, including the identification of endothelial cells, mural cells (pericytes and smooth muscle cells), inflammatory cells (**Figs. 2 and 4**) and BM-derived cells (**Fig. 5**). Staining can be performed on eye sections and on whole-mounted choroid (**Figs. 2, 3 and 4**).

Biological analyses. To evaluate the kinetics of mRNA expression using semi-quantitative RT-PCR or protein production using Western Blot, choroidal neovascularization is induced in mice with multiple argon laser burns (n=30 impacts/eye). The posterior segments (RPE-choroid complex without neural retina) are excised and immediately frozen in liquid nitrogen before RNA or protein extraction.

MATERIALS

Reagents

CRITICAL All reagents and equipment may be substituted with appropriate alternatives from other manufacturers.

- Boric acid (Aldrich, cat. no. 23.646-2)
- Carboxymethylcellulose sodium salt, medium viscosity (Sigma, cat. no. C9481-500G)
- Complete Protease inhibitor Cocktail Tablets (Roche, cat. no. 04693116001)
- Deuterium oxide 100% (EURISO-TOP, cat. no. D215ES)
- Dulbecco's Modified Eagle Medium (DMEM 1X) (Gibco, cat. no. 10938-025)
- EDTA (Merck, cat. no. 1.08418.0250)
- Eosin yellowish for microscopical staining (VWR, cat. no. 341973R)
- Ethanol 96% (VWR, cat. no. 20905.320)
- Ethanol absolute (VWR, cat. no. 20821.321)
- Ficoll (Pharmacia, cat. no. 17-0400-01)
- Fluorescein isothiocyanate (FITC)-dextran average mol wt 2,000,000 (Sigma, cat. no. FD2000S)
- Genteal® Gel (Novartis, cat. no. 1736-545)
- Glycine (Merck, cat. no. 1.04201.1000)
- Goat IgG fraction anti Guinea pig IgG – TRITC (ICN, cat. no. 55389)
- Goat anti-rat IgG Alexa Fluor 555 (Invitrogen, cat. no. A-21434)
- Guinea pig mouse anti Type IV collagen (in-house polyclonal antibody)
- Hematoxylin monohydrate for microscopy (Merck, cat. no. 1.15938.0025)
- Hydrochloric acid fuming 37% (HCl) (Merck, cat. no. 1.00317.1000)
- IGEPAL-CA 630 (Sigma-Aldrich, cat. no. I-3021)
- IsoFlo® (Abbott Laboratories, cat. no. B506), !CAUTION Toxic, use in a chemical hood.

- $K_2HPO_4.3H_2O$ (Merck, cat. no. 1.05099.1000)
- Kit for PCR amplification (e.g. Applied Biosystems, Reverse Transcriptase RNA PCR kit Thermosatble r*Tth* GeneAmp® cat. no. N808-0069)
- Kit for RNA extraction (e.g. Qiagen, RNeasy mini kit cat. no. 74103, 74101, 74106)
- Liquid Nitrogen (Air Liquide) !CAUTION Liquid nitrogen is extremely cold and can cause serious injury with severe freeze-burns, especially if splashed into the eyes or onto skin. Make sure to keep liquid nitrogen in a container designed for this purpose and wear "cryo" goggles, waterproof gloves and a waterproof apron.
- Mice: We routinely use C57BL6J mice (6-8 weeks old) and C57BL/6-GFP mice. CRITICAL It is important that mice are pigmented, with a uniformly pigmented eye fundus, to ensure the success of the laser action. The use of mosaic mice must be avoided. !CAUTION Animals of the same strain, age and sex are highly recommended unless an experiment is designed to detect variations in CNV due to these parameters. The mouse genetic background must be clearly specified because it influences CNV response. It is worth noting that because of the rd8 mutation in C57BL6/N [51], this strain may exhibit a different CNV response from C57BL6/J mice. When using transgenic or KO mice, congenic controls should be used. !CAUTION All animal studies must conform to the appropriate governmental and institutional regulations. All animal experiments described in this protocol are in accordance with the guidelines of the Animal Ethics Committee of the University of Liège (Belgium).
- Mounting medium coverquick 3000 (Labonord, cat. no. 05547537)
- N,N,N',N'-tetramethylethylendiamine (TEMED) (Sigma, cat. no. T-8133)
- NaCl (VWR, cat. no. 27810.295)
- $NaH_2PO_4.2H_2O$ (Merck, cat. no. 6345.1000)
- NaOH (UCB, cat. no. 1737)

- Optimal cutting temperature (O.C.T.) compound: Tissue-Tek O.C.T.^{TM} Compound (SAKURA, cat. no. 4583)
- Paraformaldehyde (PFA) (Sigma-Aldrich, cat. no. 441244) !CAUTION PFA is highly toxic and is irritant
- PBS (1X, prepared in-house or commercially purchased from Hyclone, cat. no. SH30028.02)
- Phosphate Buffer 0.1M (Sigma, cat. no. P7994-1EA)
- Rabbit anti rat IgG – FITC (DAKO, cat. no. F234)
- Rat anti mouse endothelial cell- CD31- PECAM-1 (PharMingen, cat. no. 553370)
- Rat anti mouse F4/80-Alexa 647 (Invitrogen, cat. no. MF48021)
- Rat anti-mouse Ly-6B.2 alloantigen (AbD serotec, cat. no. MCA771G)
- RNAse-free water (Invitrogen, cat. no. 10813-12)
- Sodium azide 99% (Janssen Chimica, cat. no. 19.038.26)
- Sodium deoxycholate (Sigma-Aldrich, cat. no. D6750-100G)
- Sodium trimethylsilyl [2,2,3,3-D_4] propionate (TSP) (EURISO-TOP, cat. no. D219PF)
- Solution NaOH, 1M (Merck, cat. no. 1.09137.1000)
- Sunitinib malate (SU-11248, LC Laboratories, Woburn, MA, cat. no. S-8803)
- Tert-amylic alcohol or $CH_3CH_2C(CH_3)_2OH$ (Merck, cat. no. 806193)
- Tetramethylrhodamine isothiocyanate-dextran (TRITC-dextran)(Sigma, cat. no. T-1287)
- Trafloxal® (ofloxacine) (Dr Mann Pharma, cat. no. 0385-658)
- Tribromo-ethilic alcohol or 2,2,2,tribromoethanol (Aldrich, cat. no. T4,840-2)
- Tris (Invitrogen, cat. no. 15504-220)
- Triton X-100 (Merck, cat. no. 1.08603.1000)
- Tropicol 0,50% (tropicamide 5mg/ml) (Thea Pharma, cat. no. 0047-894)
- Tween® (Merck, cat. no. 8.22184.0500)

- Unicaïne 0,4% (oxybuprocaini HCl 4 mg/ml) (Thea Pharma, cat. no. 0605-394)
- Vectashield mounting medium (Vector Laboratories, cat. no. H-1000)
- Xylene-CAS (Labonord cat. no. 1330-20-7) !CAUTION Xylene is a moderately hazardous compound, requiring safe handling precautions that include goggles, protective clothing, ventilation, proper gloves and storage of the material in a cool, dry and well-ventilated location because it is highly flammable.
- Xylene cyanol (Polylab, cat. no. 38505)

Equipment

- Binocular (e.g. Leitz WILD Heerbrugg M650)
- Centrifuge (e.g. Eppendorf 5415D)
- Cell strainer 70µm (e. g. BD Flacon cat. no. 352350)
- Clear disposable Base Molds 24X24 (Surgipath® cat. no. 11058624)
- Confocal microscope (e.g. Leica TCS SP2 inverted confocal laser microscope)
- Cotton swab (EMRO MEDICAL cat. no. 123011400)
- Coverslips 24X32mm (Menzel-Gläser, cat. no. 05305032)
- Cryosectionning machine (e.g. Leica CM3050S)
- Deep freezer -80°C (e.g. Froilabo BM690)
- Delicate Tissue Forceps Mod. Bonn with tying platform teeth 0.12 mm (Lawton, cat. no. 62-0255)
- E-Z Anesthesia, E-Z Systems (Corporation, Palmer USA http://www.euthanex.com)
- Edgehead Phaco Slit Knife 3.3 mm (angled) (VISITEC®, cat. no. 1109)
- Fluorescence Microscope (e.g. Olympus VANOX AHBT3)
- GraphPad Prism 5.0 (or other version, GraphPad Software)
- ImageJ64 software (National Institutes of Mental Health, http://rsb.info.nih.gov/ij/)

- Insulin syringes with sterile interior U-100 0,30mm (30G)X8mm (Becton Dickinson, Micro-fine™ , cat. no. F96071)
- Inverse NMR Cryoprobe Triple TCI (e.g. Bruker TCI)
- Iris barraquer scissors, 6 cm long, standard, 7 mm blades, sharp points (World Precision Instrument, cat. no. 14128)
- Gamma-ray Machine (e.g. Nordion, Gammacell 40 exactor, 137Cs, 662 KeV)
- Laser Photocoagulator (e.g. Alcon® Surgical Ophtalas® 532 Eyelite™)

  CRITICAL STEP Two persons are required for the laser induction, one to orientate the eye of the mouse and one to perform the laser induction.
- Luminescent image analyzer (e.g. Fujifilm Las 4000)
- MagNA Lyser Green Beads (ROCHE, cat. no. 03 358 941 001)
- MATLAB 7.9 software
- Micro Tube 2 ml, PP (Sarstedt, cat. no. 72.694.006)
- Microliter™ Syringe 5µl 75RN W/O Needle (Hamilton, cat. no. 7634-01/00)
- Microscope slides Superfrost® Plus (Menzel-Gläser, cat. no. J1800AMNZ)
- Microscope software (e.g. Olympus Cell^A 3.3, Olympus Soft imaging Solutions)
- Mini Trans-Blot Cell (Bio-Rad)
- Mini-PROTEAN Precast Gels (Bio-Rad)
- Mini-PROTEAN Tetra Electrophoresis System (Bio-Rad)
- Minicollect® Tube 0.8 mL, Z Serum Sep (Greiner, cat. no. 450472)
- NMR 5 mm Tubes for Bruker MATCH™ Holder (Hilgenberg, cat. no. 86462)
- NMR Acquisition Software (e.g. Bruker Topsin 2.1)
- NMR Analysis Software (e.g. Bruker AMIX Software version 3.9.5)
- Nuclear Magnetic Resonance Systems (e.g. Bruker AVANCE 500 MHz)
- Orbital shaker (e.g. GFL, cat. no. 3006)

- PCR Thermal Cycler (e.g. Applied Biosystems GeneAmp® PCR System 9700)
- Power supply (e.g. PowerPac 300 Bio-Rad)
- RN Needle 34G 34/10 (Hamilton, cat. no. 207434/00)
- Safe-Lock Tubes 1,5 ml (Eppendorf, cat. no. 0030 120.191)
- Safe-Lock Tubes 2,0 ml (Eppendorf, cat. no. N°0030 120.094)
- Scissors, microintraocular 25 deg (World Precision Instruments cat. no. 500372-T)
- Slit Lamp (e.g. Carl Zeiss 30SL-M)
- Spectrophotometer (e.g. Nanodrop ND-1000)
- Sterile Petri Dish 35X10 mm Style (Falcon, cat. no. 351008)
- Syringe driven Filter Unit 0.22μm (Millipore Millex®-GP)
- Syringe with needle 10ml 21G X 1 ½" (TERUMO® EUROPE, cat. no. SS-10S2138)
- Tissue Dismembrator (e.g. MagNA Lyser ROCHE)
- Tube 15 ml (Sarstedt, cat. no. 62.554.502)
- Tube 50 ml (Sarstedt, cat. no. 62.547.254)
- Vannas scissors 45 deg ang 8cm (World Precision Instruments cat. no. 500260-G)
- Vortex (e.g. IKA® minishaker MS2)
- Warming Plate (e.g. UVP®)
- Water bath up to 60°C (e.g. GFL 1083)
- Water purification system (e.g. Millipore Corporation Milli-Q 50)

Reagent setup

Paraformaldehyde (PFA) solution, 4% (wt/vol) Dissolve 4 g of paraformaldehyde in 90 ml of distilled water. Add two drops of 1 M NaOH, and mix gently overnight at room temperature (approximately 20°C). Add 10 ml of 10X PBS, and adjust to pH 7.4. Aliquot and store at -20°C until use (maximum one year).

!CAUTION PFA is highly toxic and is an irritant if exposed to skin, inhaled or swallowed. It is recommended to work with PFA in a chemical fume hood with appropriate protective gloves and safety goggles. In case of spillage, immediate cleaning is required because the powder can be easily dispersed into the air.

Equipment setup

Housing and husbandry of experimental animals. House mice under a 12-h light cycle with water and chow provided *ad libidum*. !CAUTION All experiments must be conducted in compliance with the governmental and institutional guidelines for the care and use of animals within the research program.

Laser photocoagulator. When turning on the slit lamp, ensure the slit width is at its minimum size. Set up the laser diameter at 50 μm on the slit lamp with a magnification of 30X. The power should be calibrated to 0.340 W and the exposure time set to 0.050 sec. !CAUTION The appropriate power to rupture Bruch's membrane while minimizing damage to the surrounding choriocapillaris varies with different lasers and can even change with the same laser depending upon the age of its fiber optic cable. Therefore, our recommendations for power settings are suggestions, and the laser output must be calibrated. For laser calibration, perform burns on the retina of a "calibration mouse" starting with relatively low power and gradually increasing until the lowest power that reproducibly ruptures Bruch's membrane is identified with the creation of a bubble. A major pitfall is using too much power, which damages the surrounding choriocapillaris and reduces or completely prevents choroidal neovascularization. !CAUTION Check that the Dr Filter is switched to ON to protect the operator from laser reflection. !CAUTION Do not look at the laser flash. Any laser beam reflection on any glass surface may damage the retina.

PROCEDURE

BM transplant (optional). TIMING 1 day for transplantation and 5 weeks for BM restoration

CRITICAL This section must be performed 5 weeks before laser induction to allow BM reconstruction.

CRITICAL This section must be performed by licensed and qualified individuals according to institutional guidelines.

CRITICAL This section must be performed under sterile conditions.

1. Irradiate recipient mice (8-10 weeks old) with a single dose of 9 Gy.
2. Sacrifice donor mice (8-10 weeks of age) by cervical dislocation (or in accordance with the local animal use committee).
3. Remove both posterior limbs with scissors. Remove as much hair, skin and muscle as possible without compromising the marrow cavity. Remove a portion of the pelvic bone if necessary.
4. Place approximately 8 ml of culture medium in a 10-cm diameter culture dish.
5. Thoroughly scrap the tibia and femur of all fascia, connective tissue and muscle. Separate bones at the knee joint. Store bones in medium until all bones are collected for the next step (maximum 1hour).
6. Carefully clip the epiphysis and distal ends of each bone. Using approximately 2 ml of medium, slowly flush BM with a 27-gauge needle into a tube.
7. Dissociate cell aggregates using a pipette, and pass the cell suspension through a 70-μm cell strainer.
8. Count the total number of cells using a Thoma slide.
9. Inject BM cells (10^7 per animal) i.v. into irradiated recipient mice (from step 1).

10. If using GFP donor mice, confirm BM restoration after 5 weeks by analyzing the proportion of GFP+ cells in blood and BM samples via flow cytometry (approximately 75% restoration should be achieved). Alternatively, confirm BM cross-transplantation by genotyping the BM.

Material preparation and laser induction

TIMING 45 min for 12 mice

11. Place the slit lamp where it is easily accessible to both users, and place the mouse support on the chin rest.

CRITICAL STEP Before any manipulation, confirm the health of the mice's eyes macroscopically, and discard any mouse with a cataract or visible defect of the cornea, which diminishes eye clarity.

CRITICAL STEP Pre-warm the warming plate to 34°C before the procedure to be ready after laser induction to lay the mice on it until awakening to prevent hypothermia due to anesthesia.

12. Anesthetize the mouse by i.p. injection of avertine at an appropriate dose (i.e., use 350 μl for a 20-g mouse). Anesthesia is effective for 30-40 min, and complete awakening occurs after 2 h.

CRITICAL STEP This step must be performed by licensed and qualified individuals according to institutional guidelines.

13. Wait 2-5 min until the mouse is fully anesthetized.

14. Place a drop of tropicamide in each eye of each mouse to dilate the pupils.

15. Wait 3-5 min until pupils are completely dilated before placing the mouse on a pre-warmed mouse support for laser induction.

16. Confirm pupil dilatation.

CRITICAL STEP The pupils must be completely dilated to see the entire eye fundus.

17. Place the mouse on the support for laser induction (mouse operator). CRITICAL STEP This and the following X steps requires two researchers, the first, the mouse operator (MO) manipulates the mouse, and the second, the laser operator (LO) performs the laser induction.

18. Set the height of the mouse support with the chin rest adjuster to place the mouse's eye in front of the laser beam (LO).

19. Place the mouse perpendicular to the laser beam and protrude the eye completely to position the eye for laser induction (MO).

CRITICAL STEP The eye must be well deorbited to facilitate impact positioning.

20. Place a drop of GenTeal® (or Goniosol) on the corner of a coverslip and place it carefully on the eye as a contact lens to convert the curved surface of the cornea to a planar surface (MO).

CRITICAL STEP To prevent eye immobilization, do not put too much pressure on the cover glass.

!CAUTION For operator safety and to prevent laser beam reflection towards the LO, do not place the cover glass perpendicularly.

21. Confirm that the cover glass is in place and acts as a contact lens. The mouse is now ready for laser induction (LO).

22. Switch on the laser photocoagulator and focus the laser beam on the retinal pigmented epithelium of the eye fundus (LO).

!CAUTION Visualize the retina and precisely focus the aiming beam on the retina before activating the laser. Defocusing the aiming beam could lead to burns that do not rupture Bruch's membrane and fail to yield CNV.

23. Induce 4 impacts (at the noon, 3, 6 and 9 o'clock positions) or more impacts (i.e., 30-40 impacts) around the optic nerve using the laser's trigger pedal (LO).

!CAUTION Do not look at the laser flash. The laser beam's reflection on the cover glass may cause damage to the retina.

CRITICAL STEP A bubble should appear, confirming the efficiency of laser induction (Supplemental video 1). Only burns that produce a bubble should be included in the study.

CRITICAL STEP Avoid laser impacts to the retinal vessels to prevent intraocular hemorrhage.

24. After laser induction, lay the mouse on the warming plate until awakening to prevent hypothermia due to anesthesia. If necessary proceed the following steps whilst the mouse is still under anesthesia.

Mouse treatment (optional) TIMING less than 3 min per mouse, per treatment

25. If desired, perform intraperitoneal (i.p.; option A) or intravitreous (i.v.; option B) injections.

A) I.p. injection.

i) Perform a single injection during or after anesthesia. If required, several injections may be performed during mouse housing.

CRITICAL STEP This step must be performed by licensed and qualified individuals according to institutional guidelines.

B) intravitreous (i.v.) injections (i) Prepare 2 μl of the drug in a Hamilton syringe with a 34G needle.

(ii) Place the mouse under the microscope.

(iii) Apply one drop of local anesthetic (e.g., Unicaïne 0.4%) on the eye surface and dry the excess liquid.

(iv) Gently protrude the mouse eye.

(v) Use a 30G needle to puncture the sclera 1 mm from the limbus. Hold the needle vertical to the scleral surface, and only insert the tip of the needle. Some vitreous will leak

from the puncture hole. CRITICAL STEP This injection must be performed under an operation microscope directly after laser induction when the mice are still under anesthesia. CRITICAL STEP This step must be performed by licensed and qualified individuals according to institutional guidelines.

CRITICAL STEP A complement to anesthesia is given to awakening mice. (i.p. injection of anesthetic at an appropriate dose in accordance with the local animal use committee, for instance, use 100 μl of avertine for a 20-g mouse that already received 350μl)

(vi) Gently press on the eye with a cotton swab to extrude more vitreous and gain volume in the posterior chamber for drug injection.

(vii) Insert the 34G needle of a Hamilton syringe through the puncture hole at a 45° angle relative to the scleral surface.

CRITICAL STEP. Avoid injuring the lens with the needle, which can lead to secondary cataracts.

CRITICAL STEP Prevent any bleeding, which can lead to infection.

CRITICAL STEP Do not inject air bubbles into the vitreous.

(viii) Slowly inject 2 μl of the drug into the posterior chamber of the mouse eye, and wait a few seconds before removing the needle from the eye.

CRITICAL STEP Take care to maneuver around the lens, and avoid delivering the solution close to the retina.

(ix) Wait a few seconds before removing the needle from the eye.

(x) Apply an antibiotic ointment (oxofloxacine, 3 mg/g) (e.g., Trafloxal®) to the eye surface to prevent infection.

(xi) Lay the mouse on the warming plate until it awakens.

Mouse sacrifice and enucleation

TIMING 5-10 min per mouse

26. If vascularization analysis is required on flat-mounted choroids, inject one mouse with FITC-dextran, anesthetize the mouse as described in Step 12, perfuse the mouse with PBS (0.2 ml) containing FITC-dextran (5 mg/ml) and wait for 3 minutes. Alternatively proceed direct to the next step.

CRITICAL STEP Prepare FITC-dextran immediately before use.

27 Sacrifice the mouse by cervical dislocation (or in accordance with the local animal use committee).

CRITICAL STEP This step must be performed by licensed and qualified individuals according to institutional guidelines.

28 Collect intracardiac blood if needed and store in a Minicollect Tube for Serum separation. Centrifuge the tube for 10 min at 1500g. Serum may be stored in microtubes at -80°C for several months.

29 Perform enucleation. Insert Vannas scissors along the eye into the orbital cavity and section the four optical muscles and the optic nerve, which appears as a white cord behind the eye. Harvest the eye and remove excess periocular muscles in PBS (Supplemental video 2).

CRITICAL STEP Perform steps 26-29 on one mouse at a time. Do not perform these steps on several mice simultaneously.

Eye storage and preparation

30 Embed eyes in O.C.T. compound (option A) for histological analyses, freeze eyes for protein or RNA extraction (option B) or flat-mount the choroids for whole-mount analyses (option C).

(A) Embedding of eyes in O.C.T. compound for cryosectioning.

TIMING 3-5 min per eye

(i) Embed eyes in O.C.T. compound. First, add a small quantity of O.C.T. to an aluminum cryomold. Next, place the eye into the cryomold with its optic nerve-pupil axis oriented horizontally. Finally, fill the cryomold with O.C.T. compound.

(ii) Freeze in liquid nitrogen vapor, and store immediately at -80°C.

CRITICAL STEP To prevent histological damage, do not immerse the sample in liquid nitrogen.

PAUSE POINT Blocks may be stored until cryostat sectioning, but it is preferable to analyze them within 6 months.

(B) Cryopreservation of eyes

TIMING less than 1 min

(ii) Freeze the eye directly in liquid nitrogen.

(iii) Store in a cryotube at -80°C.

PAUSE POINT Frozen eyes may be stored until needed for protein or RNA extraction.

(C) Choroid flat-mounting

TIMING 1 day

(i) Fix eyes in 1 ml of 1% PFA for 1-2 h at room temperature.

(ii) Dissect the cornea and lens (Supplemental video 3).

(iii) Carefully remove the entire retina from the eyecup.

CRITICAL STEP The retina must be fully removed; otherwise, artifactual vessels may be observed.

(iv) Perform 4-8 radial cuts from the edge to the equator.

CRITICAL STEP Cut between laser impacts. Take care to keep the neovascular membrane intact.

CRITICAL STEP To perform basic immunofluorescence on a flat-mounted choroid, proceed immediately to step 31 option C.

(v) If you are not staining, mount flat-mounted choroids with VECTASHIELD medium, and store in the dark at +4°C for several weeks.

PAUSE POINT Flat-mounted choroids may be stored for several weeks, but it is preferable to analyze them immediately.

Staining and imaging, RNA and protein analysis.

31) Stain samples using hematoxylin-eosin staining (option A on 6µm cryosections of O.C.T. embedded eyes) or immunofluorescence (option B on 6µm cryosections of O.C.T. embedded eyes and option C on whole mount samples). Alternatively, according to your particular experiment, proceed to mRNA (option D) or protein extraction (option E) from the posterior segments (RPE-choroid complex without neural retina) that have been frozen in liquid nitrogen (step 30B).

A) Hematoxylin-eosin staining

TIMING 1 h

(i) Fix samples in 4% PFA for 10 min.

(ii) Wash twice for 15 min in xylene.

(iii) Successively rehydrate for 2 min in absolute ethanol, 95% ethanol, 70% ethanol and distilled water.

(iv) Stain slides for 8 min in a hematoxylin bath followed by an 8-min wash with tap water.

(v) Counterstain with eosin for 30 seconds.

(vi) Dehydrate rapidly in successive baths of distilled water, 70% ethanol, 95% ethanol and absolute ethanol for 2 min.

(vii) Wash slides in two baths of xylene for 2 min.

(viii) Mount slides with a resin (e.g., Coverquick mounting medium).

(B) Basic immunofluorescent protocol for cryostat sections

TIMING 4 h

(i) Cut 6-μm-thick sections on a cryostat.

(ii) Fix in acetone at -20°C for 2 min and then in methanol at +4°C for 5 min.

(iii) Block sections in PBS containing 10% bovine serum albumin for 1 h at room temperature. Next, incubate the sections with a primary antibody specific to the protein of interest, such as 1 h at room temperature with a rat monoclonal antibody raised against mouse platelet endothelial cell adhesion molecule (PECAM) (diluted 1/20) or an in-house guinea pig polyclonal antibody raised against mouse type IV collagen (diluted 1/100).

(iv) Wash tissue sections three times for 10 min in PBS.

(v) Incubate for 30 min in the dark with the appropriate secondary antibodies, such as FITC-conjugated rabbit anti-rat IgG (diluted 1/40) or TRITC-conjugated goat IgG fraction anti-guinea pig (diluted 1/40).

(vi) Wash sections three times for 10 min with PBS, and rinse in 10 mM Tris-HCl buffer (pH 8.8).

(vii) Mount under a coverslip with VECTASHIELD, and visualize sections under an inverted microscope equipped with epifluorescence optics.

(C) Basic immunofluorescent protocol for whole mounts

TIMING 3 h over 2 days

(i) Wash in PBS for 30 min under agitation.

(ii) Store in PBS containing sodium azide (1%) at 4°C in 24-well plates for maximum 2 days.

(iii) Wash in PBS and then block with PBS containing 10% bovine serum albumin for 1 h under agitation at room temperature. If using fresh choroids, proceed directly to blocking.

(iv) Incubate overnight under agitation at room temperature with a primary antibody specific to the protein of interest, such as Alexa 647-conjugated mouse F4/80 (diluted 1/100) or rat anti-mouse Ly-6B.2 (diluted 1/100).

(v) After three washes for 20 min in PBS under agitation, incubate with the appropriate secondary antibodies (for example, Alexa Fluor 555-conjugatred goat anti-rat IgG (Invitrogen; cat no A-21434; diluted 1/1000) for 90 min.

(vi) Wash three times for 20 min under agitation in PBS, and mount in mounting medium.

D) mRNA extraction (TIMING 1 half-day)

i) Extract total RNA under RNase-free conditions using an RNeasy extraction kit (Qiagen) after homogenization of tissue extracts by placing posterior segments in tubes containing ceramic beads (MagNA Lyser Green Beads) and Lysis Buffer (from the RNeasy extraction kit) in the MagNA Lyser according to the manufacturer's protocol (QIAGEN RNeasy mini kit).

PAUSEPOINT Store RNA at -80°C until use (for maximum two years).

E) Protein extraction (TIMING half-day for each, 20 min for metabolomics)

i) lyse samples for 30 min in ice-cold lysis buffer (1% Triton X-100, 150 mM NaCl, 1% IGEPAL-CA 630, 1% sodium deoxycholate, 0.1% SDS, complete).

ii) To homogenize, place tissue extracts in tubes containing ceramic beads (MagNA Lyser Green Beads) in a MagNA Lyser at 6500 rpm for 45 seconds.

iii) Clarify cell lysates by centrifugation at 12,000 g at 4°C for 15 min.

PAUSEPOINT Store proteins at -20°C until use (for maximum one year).

Image Analysis (optional)

32 Analyze neoformed vessels in laser-induced lesions as appropriate for your particular experiment. Quantification may be performed on tissue sections (option A) or on flat-mounted choroids in 2D (option B) or 3D (option C).

(A) Assessment of neovascular lesion thickness by estimating the B/C ratio in tissue sections

TIMING 1 half-day

(i) Capture a microscopic image (working magnification: 200X) of a hematoxylin-eosin-stained eye section with a video camera.

(ii) Use ImageJ to measure the thickness of the lesion from the bottom of the pigmented choroidal layer to the top of the neovascular membrane (B) and the thickness of the intact pigmented choroid adjacent to the lesion (C) (**Fig. 2a**).

(iii) Determine the B/C ratio.

CRITICAL STEP For this analysis, cut frozen serial sections throughout the extent of each CNV lesion induced by laser impact. Quantify at least 5 sections per lesion/impact for all impacts.

(B) 2D quantification of the neovascular area on flat-mounted choroids

TIMING 1 half-day

(i) Visualize slides on an epifluorescence or confocal microscope.

(ii) Digitize images captured with a three-color video camera.

(iii) Use ImageJ to measure the total area (in μm^2) of the CNV lesion (**Fig. 2d-g**).

(iv) Set scale on a reference slide with a scale in ImageJ.

(v) Open the original Red-Green-Blue color picture in ImageJ (**Fig. 2d**).

(vi) Select the blood vessel area, and erase the background of the original picture (**Fig. 2e**).

(vii) Extract the green component of the picture (**Fig. 2f**).

(viii) Quantify the pixels (in red in the figure) using ImageJ after application of the threshold to select blood vessel structures (**Fig. 2 g**).

CRITICAL STEP Take a calibration image from a slide with a grating of known size.

Use an established and constant threshold in pixels (corresponding to threshold fluorescence) to quantify neovascularization.

(ix) Determine a mask for the CNV area using the image analysis module of ImageJ.

(x) Binarize images using a threshold that covers the entire vasculature of the CNV.

(xi) Measure the fluorescent vessel area.

(C) 3D quantification of the neovascular volume on flat-mounted choroids

TIMING 5 minutes/impact for image acquisition

(i) Visualize slides with a confocal laser microscope equipped with a multi-argon laser (for FITC) and two helium-neon lasers (a HeNe of 561 nm for TRITC Alexa Fluor 555 and a HeNe of 633 nm for Alexa Fluor 647).

(ii) Digitize the images acquired using a 20X (NA 0.7) Plan-Apo objective at 1024 X 1024-pixel resolution. For multicolor imaging, use the following filters for the indicated fluorophores: FITC, excitation at 488 nm and emission at 500-535 nm; TRITC, excitation at 561 nm and emission at 570-600 nm; Alexa 555, excitation at 561 nm and emission at 568-600 nm; and Alexa 647, excitation at 633 nm and emission at 640-700 nm.

(iii) For each lesion, record serial optical sections with a *z*-step of 0.99 μm.

(iv) Construct 3D images using confocal software.

(v) Determine the CNV volume using the image analysis toolbox in MATLAB 7.9.

Metabolomics (optional)

33) Add 500 μl of D2O (deuterium oxide or heavy water) phosphate buffer (0.1 M, pH 7.4) supplemented with 30 μl of TSP (sodium trimethylsilyl[2,2,3,3-D4]propionate) solution in D2O (10 mg/ml) to mouse serum (200 μl) (see step 28).

CRITICAL STEP A minimum of 5 samples per condition must be analyzed to obtain relevant data.

i) Place the samples in 5-mm NMR capillaries (Bruker Match system) for data acquisition.

ii) Acquire one-dimensional 1H-NMR spectra at 25°C on a Bruker Avance spectrometer operating at 500.13 MHz with a BBI probe. Apply the Carr-Purcell-Meiboom-Gill sequence with water pre-saturation to attenuate broad signals arising from proteins and lipoproteins and the water signal. Adjust the fixed echo time (tD) to 300 ms, and set the loop number to 64. Collect 128 transients. Acquisition parameters include a 90° pulse, 64k time domain points, a spectral width of 10,000 Hz, an acquisition time of 3.277 s and a relaxation delay of 4 s. Prior to Fourier transformation (FT), zero-fill the free induction decays (FIDs) to 128k. Phase and baseline correct all spectra, and set the TSP resonance to 0.00 ppm.

CRITICAL STEP Pay particular attention to the Shims setup.

iii) Reduce the optimized 1H-NMR spectra to ASCII files using AMIX (Bruker, version 3.9.5). Normalize peak intensities to total intensities and reduce to 0.04-ppm integrated regions (buckets).

CRITICAL STEP Remove the regions between 4.5 and 5.5 ppm and between 0 ppm and 0.5 ppm prior to statistical analysis because of the presence of water and of the internal standard TSP.

iv) Perform principal component analysis (PCA) using AMIX (Bruker, version 3.9.5) with Pareto scaling of bucket variables.

TIMING

Step 1-10: BM transplantation: 1 d for transplantation and 5 w for BM restoration.

Steps 11-24: Material preparation and laser induction: 45 min for 12 mice.

Steps 25: Mouse injections: 1-6 min per mouse, depending on the mode of injection.

Steps 26-29: Mouse sacrifice and enucleation: 5-10 min.

Step 30: Eye storage and preparation: from 5 min for OCT storage to 1 day for flat-mounted choroid preparation.

Step 31: Hematoxylin-eosin staining: 1 h.

Step 31: Immunostaining: 4 h (option A) or 3 h over 2 days (option B).

Steps 31: mRNA and protein analysis: 1 half-day for each.

Step 32: Image Analysis of neoformed vessels: 1 half-day (option A), 1 half-day (option B) or 1 day (option C).

Step 33: Metabolomics study: 20 min per sample and 2 h for statistical analysis.

TROUBLESHOOTING

See Table 1 for Troubleshooting guidance.

ANTICIPATED RESULTS

The development of neovascular lesions over time can be evaluated in a typical experiment in which laser burn-induced lesion are determined at different time points (Fig.3). CNV is expected to take place within 5 days. At day 7, a typical mushroom-like lesion is observed with a regression of neo-formed blood vessels from day 21. Inflammatory cells rapidly infiltrate the CNV lesion with a neutrophil peak at day 1 to 3, followed by a macrophage one at day 5. Inflammatory cells are no longer detected at day 7 (Fig. 4).

An illustrative assay using a tyrosine kinase inhibitor (sunitinib) [52] is shown in Fig. 5a. The CNV surface measurement reveals a drastic reduction of vessel formation upon oral administration of the anti-angiogenic inhibitor (Fig. 5a). Examples of CNV quantifications by the determination of B/C ratio on eye section (Fig 5b), CNV area (Fig 5c) and CNV volume (Fig 5d and supplemental video 4) on flat mounted choroid (Fig; 5c) are shown by applying the model to MMP13-deficient mice. This experiment also emphasizes the interest to use genetically modified mice in order to unravel molecular mechanism underlying AMD [8, 19, 24-28, 53, 54]. BM-derived cell recruitment within the choroidal lesion is demonstrated by the

transplantation of BM isolated from GFP-transgenic mice into C57Bl/6J mice (Fig. 5 e-f) [5, 49, 50].

^{1}H-NMR metabolomics approach emerged recently as a powerful method to identify changes in small molecular weight organic molecules (metabolites) associated to pathologies [55-58]. This method is suitable to discriminate mice displaying different angiogenic response. A proof-of-principle is shown in a MicroRNA (miRNA) study demonstrating CNV reduction through pre-miR administration (e.g. miR21, a miR with anti-angiogenic activity) [13](Fig. 6). In this assay, 4 different animal groups are discriminated: (i) control mice not subjected to laser and not injected (group 1), (ii) mice subjected to laser and either non injected (group 2) or injected with scramble pre-miR (group 3), and (iii) laser-induced mice injected with pre-miR21 (group 4).

ACKNOWLEDGMENTS

This work was supported by grants from the Fonds de la Recherche Scientifique - FNRS (F.R.S.-FNRS, Belgium), the Foundation against Cancer (foundation of public interest, Belgium), the Fonds spéciaux de la Recherche (University of Liège), the Direction Générale Opérationnelle de l'Economie, de l'Emploi et de la Recherche from the S.P.W. (Région Wallonne, Belgium), the Interuniversity Attraction Poles Programme - Belgian Science Policy (Brussels, Belgium), the Plan National Cancer (Service Public Fédéral), the Actions de Recherche Concertées (University of Liege, Belgium).

The authors thank Sandra Ormenese and Gustavo Moraes from the GIGA Cell Imaging and Flow Cytometry facility their support with confocal microscopy acquisitions, as well as the GIGA-animal facility platform for their help.

AUTHOR CONTRIBUTIONS

VL set up the assay CNV, collected data and compiled the protocol with input from the authors. JL performed the optimization of BM transplantation and conducted the assay with knock-out mice. SH carried out immunostainings. SB develops the methods of quantification. MLAG contributed to the set up of intravitreal injection. IS conducted the assays with mir21. NES conducted the assays with Sunitinib. PdT performed metabolomics study. ER designed statistical analysis. JMF and JMR contributed to the design of the study and critically evaluated the manuscript. AN designed the assays and wrote the manuscript. All authors revised the manuscript.

COMPETING FINANCIAL INTERESTS

The authors declare no competing financial interests.

LEGENDS OF FIGURES

Figure 1: Overview of the procedure. The general protocol for CNV induction involves mouse preparation followed by CNV induction, experimental treatment or use of transgenic mice, sacrifice and enucleation, sample preparation and analysis. The different steps described in the text are indicated on the left.

Figure 2: Methods of 2D quantifications of the choroidal lesion. (a) A typical section of laser burned eye stained with Hematoxylin-eosin, with the lesion delineated by the dotted line. The bold bars indicate the total thickness from the bottom of the choroid to the top of the lesion (B, black bar) and the thickness of adjacent normal choroid (C, white bar). The neovascular reaction is quantified by determining the B/C ratio. (b) Staining of a typical lesion delineated by the dotted line with anti-PECAM (in red) and anti-type IV collagen (coll IV) (in green). (c) The advantage of the B/C quantification (quantitative morphometric assessment of

neovascular lesion thickness) method (over surface estimation) is its independence in relation to oblique sections. (d-g) A typical image of FITC-dextran labeled blood vessels on flat mounted choroid. (d) Original Red-Green-Blue color picture of a neovascular membrane on flat mounted choroid. (e) The selection of the blood vessel area using imageJ erases the background from the original picture. (f) Extraction of the green component. (g) Quantification is realized by binarization of the impact using ImageJ after selection of the threshold to mainly select blood vessel structures (shown in red in the picture). R: Retina, CH: choroid, S: sclera.

Figure 3: FITC-dextran labeled flat mounted choroid at different times after laser induction. (a-f) Illustration of a representative flat mounted choroid labeled with FITC-dextran at day 1 to day 21. The dotted line delineates the lesion. (g) Quantification of the area of fluorescent neovessels by computerized analysis with imageJ software.

Figure 4: Immunostaining for inflammatory cells on flat mounted choroid collected at different time points after laser induction. (a-d) Labeling of macrophages in red with F4/80 at day 1, 3, 5 and 7. (e-h) Staining of neutrophils in red with Ly-6B.2 at day 1, 3, 5 and 7. Neutrophils are detected earlier (days 1 and 3) than macrophages (day 5).

Figure 5: Typical analyses of laser-induced CNV in mice. (a) The treatment *per os* with Sunitinib malate (SU-11248) 40mg/kg during 7 days significantly decreases the neovessel area as compare to control (CTL) group treated with vehicle (0.5% carboxymethylcellulose) alone. (b-d) The MMP-13 deficiency in mice impairs the choroidal neovascularization as demonstrated by B/C ratio (b), vessel area (c) and volume (d) on flat mounted choroids. (e-f) BM cells issued from GFP mice (in green) and transplanted into BL6 mice are recruited in

CNV lesions labeled with TRITC-Dextran (in red) after 7 (D7) and 14 (D14) days. (KO: *Mmp13*-/- mice; WT: wild-type *Mmp13*+/+ mice

Figure 6: Metabolomics (MBX) analysis of sera collected from mice subjected or not to laser induction and injected or not injected with pre-miR. The Principal Component Analysis (PCA) leads to the discrimination of the different groups. The PCA score plot (principal component 1 (PC1) *vs* principal component 2 (PC2)) illustrates the differentiation of the groups: sera from CNV laser induced mice without injection (■), CNV laser induced mice with scramble pre-miR injection (▲) and CNV laser induced mice with pre-miR21 injection (●) vs control mice (✖). MBX analysis highlights the impact of CNV on the metabolism and corroborates the positive effect of pre-miR injection on the laser induced CNV.

Supplemental video 1: Laser burn induction with the apparition of a bubble, which confirms the efficiency of the laser impact.

Supplemental video 2: Eye is properly cleaned by removing muscles in excess and the optic nerve. Some conjunctive tissues are left close to the limbus to facilitate the eye grip during the dissection.

Supplemental video 3: Cornea and retina are gently removed. The sclera-choroid complex is turned upside down and cut between the laser impacts. Choroid is placed on a microscopic slide, mounted medium (Vectashield) is put down and a coverslip is placed on the flat mounted choroid.

Supplemental video 4: Illustration of a 3D reconstruction of laser impact after confocal imaging.

REFERENCES

1. Resnikoff, S. et al. Global data on visual impairment in the year 2002. *Bulletin of the World Health Organization* **82**, 844-51 (2004).
2. Friedman, D.S. et al. Prevalence of age-related macular degeneration in the United States. *Archives of ophthalmology* **122**, 564-72 (2004).
3. de Jong, P.T. Age-related macular degeneration. *The New England journal of medicine* **355**, 1474-85 (2006).
4. Miller, J.W. Age-related macular degeneration revisited--piecing the puzzle: the LXIX Edward Jackson memorial lecture. *American journal of ophthalmology* **155**, 1-35 e13 (2013).
5. Jost, M. et al. Tumoral and choroidal vascularization: differential cellular mechanisms involving plasminogen activator inhibitor type I. *Am J Pathol* **171**, 1369-80 (2007).
6. Noel, A., Jost, M., Lambert, V., Lecomte, J. & Rakic, J.M. Anti-angiogenic therapy of exudative age-related macular degeneration: current progress and emerging concepts. *Trends Mol Med* **13**, 345-52 (2007).
7. Pennesi, M.E., Neuringer, M. & Courtney, R.J. Animal models of age related macular degeneration. *Molecular aspects of medicine* **33**, 487-509 (2012).
8. Tobe, T. et al. Targeted disruption of the FGF2 gene does not prevent choroidal neovascularization in a murine model. *The American journal of pathology* **153**, 1641-6 (1998).
9. Saishin, Y. et al. VEGF-TRAP(R1R2) suppresses choroidal neovascularization and VEGF-induced breakdown of the blood-retinal barrier. *Journal of cellular physiology* **195**, 241-8 (2003).

10. Heier, J.S. et al. Intravitreal aflibercept (VEGF trap-eye) in wet age-related macular degeneration. *Ophthalmology* **119**, 2537-48 (2012).

11. Slakter, J.S. Anecortave acetate for treating or preventing choroidal neovascularization. *Ophthalmology clinics of North America* **19**, 373-80 (2006).

12. Slakter, J.S. et al. Anecortave acetate (15 milligrams) versus photodynamic therapy for treatment of subfoveal neovascularization in age-related macular degeneration. *Ophthalmology* **113**, 3-13 (2006).

13. Sabatel, C. et al. MicroRNA-21 exhibits antiangiogenic function by targeting RhoB expression in endothelial cells. *PLoS One* **6**, e16979 (2011).

14. Shi, Y.Y. et al. Monocyte/macrophages promote vasculogenesis in choroidal neovascularization in mice by stimulating SDF-1 expression in RPE cells. *Graefe's archive for clinical and experimental ophthalmology = Albrecht von Graefes Archiv fur klinische und experimentelle Ophthalmologie* **249**, 1667-79 (2011).

15. Apte, R.S., Richter, J., Herndon, J. & Ferguson, T.A. Macrophages inhibit neovascularization in a murine model of age-related macular degeneration. *PLoS medicine* **3**, e310 (2006).

16. Zhou, J. et al. Neutrophils promote experimental choroidal neovascularization. *Molecular vision* **11**, 414-24 (2005).

17. Machalinska, A. et al. Neural stem/progenitor cells circulating in peripheral blood of patients with neovascular form of AMD: a novel view on pathophysiology. *Graefe's archive for clinical and experimental ophthalmology = Albrecht von Graefes Archiv fur klinische und experimentelle Ophthalmologie* **249**, 1785-94 (2011).

18. Wang, J. et al. Amyloid beta enhances migration of endothelial progenitor cells by upregulating CX3CR1 in response to fractalkine, which may be associated with

development of choroidal neovascularization. *Arteriosclerosis, thrombosis, and vascular biology* **31**, e11-8 (2011).

19. Lecomte, J. et al. Bone marrow-derived mesenchymal cells and MMP13 contribute to experimental choroidal neovascularization. *Cellular and molecular life sciences : CMLS* **68**, 677-86 (2011).
20. Zhou, B. & Wang, B. Pegaptanib for the treatment of age-related macular degeneration. *Experimental eye research* **83**, 615-9 (2006).
21. Rosenfeld, P.J., Rich, R.M. & Lalwani, G.A. Ranibizumab: Phase III clinical trial results. *Ophthalmology clinics of North America* **19**, 361-72 (2006).
22. Lien, S. & Lowman, H.B. Therapeutic anti-VEGF antibodies. *Handbook of experimental pharmacology*, 131-50 (2008).
23. Van de Veire, S. et al. Further pharmacological and genetic evidence for the efficacy of PlGF inhibition in cancer and eye disease. *Cell* **141**, 178-90 (2010).
24. Rakic, J.M. et al. Placental growth factor, a member of the VEGF family, contributes to the development of choroidal neovascularization. *Invest Ophthalmol Vis Sci* **44**, 3186-93 (2003).
25. Lambert, V. et al. MMP-2 and MMP-9 synergize in promoting choroidal neovascularization. *FASEB J* **17**, 2290-2 (2003).
26. Lambert, V. et al. Influence of plasminogen activator inhibitor type 1 on choroidal neovascularization. *FASEB J* **15**, 1021-7 (2001).
27. Lambert, V. et al. Dose-dependent modulation of choroidal neovascularization by plasminogen activator inhibitor type I: implications for clinical trials. *Invest Ophthalmol Vis Sci* **44**, 2791-7 (2003).

28. Rakic, J.M. et al. Mice without uPA, tPA, or plasminogen genes are resistant to experimental choroidal neovascularization. *Invest Ophthalmol Vis Sci* **44**, 1732-9 (2003).

29. Liu, J. et al. Relationship between complement membrane attack complex, chemokine (C-C motif) ligand 2 (CCL2) and vascular endothelial growth factor in mouse model of laser-induced choroidal neovascularization. *The Journal of biological chemistry* **286**, 20991-1001 (2011).

30. Lyzogubov, V.V. et al. Role of ocular complement factor H in a murine model of choroidal neovascularization. *The American journal of pathology* **177**, 1870-80 (2010).

31. Malek, G. et al. Apolipoprotein E allele-dependent pathogenesis: a model for age-related retinal degeneration. *Proceedings of the National Academy of Sciences of the United States of America* **102**, 11900-5 (2005).

32. Imamura, Y. et al. Drusen, choroidal neovascularization, and retinal pigment epithelium dysfunction in SOD1-deficient mice: a model of age-related macular degeneration. *Proceedings of the National Academy of Sciences of the United States of America* **103**, 11282-7 (2006).

33. Sengupta, N. et al. Paracrine modulation of CXCR4 by IGF-1 and VEGF: implications for choroidal neovascularization. *Investigative ophthalmology & visual science* **51**, 2697-704 (2010).

34. Qi, X. et al. gamma-Secretase inhibition of murine choroidal neovascularization is associated with reduction of superoxide and proinflammatory cytokines. *Investigative ophthalmology & visual science* **53**, 574-85 (2012).

35. Luo, L. et al. Targeted intraceptor nanoparticle therapy reduces angiogenesis and fibrosis in primate and murine macular degeneration. *ACS nano* **7**, 3264-75 (2013).

36. Hasegawa, E. et al. IL-27 inhibits pathophysiological intraocular neovascularization due to laser burn. *Journal of leukocyte biology* **91**, 267-73 (2012).

37. Halkein, J. et al. MicroRNA-146a is a therapeutic target and biomarker for peripartum cardiomyopathy. *The Journal of clinical investigation* **123**, 2143-54 (2013).

38. Espinosa-Heidmann, D.G. et al. Macrophage depletion diminishes lesion size and severity in experimental choroidal neovascularization. *Invest Ophthalmol Vis Sci* **44**, 3586-92 (2003).

39. Sakurai, E., Anand, A., Ambati, B.K., van Rooijen, N. & Ambati, J. Macrophage depletion inhibits experimental choroidal neovascularization. *Invest Ophthalmol Vis Sci* **44**, 3578-85 (2003).

40. Campochiaro, P.A. The complexity of animal model generation for complex diseases. *JAMA : the journal of the American Medical Association* **303**, 657-8 (2010).

41. Kwak, N., Okamoto, N., Wood, J.M. & Campochiaro, P.A. VEGF is major stimulator in model of choroidal neovascularization. *Investigative ophthalmology & visual science* **41**, 3158-64 (2000).

42. Miki, K. et al. Effects of intraocular ranibizumab and bevacizumab in transgenic mice expressing human vascular endothelial growth factor. *Ophthalmology* **116**, 1748-54 (2009).

43. Espinosa-Heidmann, D.G. et al. Age as an independent risk factor for severity of experimental choroidal neovascularization. *Investigative ophthalmology & visual science* **43**, 1567-73 (2002).

44. Espinosa-Heidmann, D.G. et al. Gender and estrogen supplementation increases severity of experimental choroidal neovascularization. *Experimental eye research* **80**, 413-23 (2005).

45. Ridder, W., 3rd, Nusinowitz, S. & Heckenlively, J.R. Causes of cataract development in anesthetized mice. *Experimental eye research* **75**, 365-70 (2002).

46. Mori, K. et al. Pigment epithelium-derived factor inhibits retinal and choroidal neovascularization. *Journal of cellular physiology* **188**, 253-63 (2001).

47. Tomida, D. et al. Suppression of choroidal neovascularization and quantitative and qualitative inhibition of VEGF and CCL2 by heparin. *Investigative ophthalmology & visual science* **52**, 3193-9 (2011).

48. Takahashi, H. et al. Contribution of bone-marrow-derived cells to choroidal neovascularization. *Biochemical and biophysical research communications* **320**, 372-5 (2004).

49. Sengupta, N. et al. The role of adult bone marrow-derived stem cells in choroidal neovascularization. *Investigative ophthalmology & visual science* **44**, 4908-13 (2003).

50. Tomita, M. et al. Choroidal neovascularization is provided by bone marrow cells. *Stem cells* **22**, 21-6 (2004).

51. Chen, M. et al. Age- and light-dependent development of localised retinal atrophy in CCL2(-/-)CX3CR1(GFP/GFP) mice. *PLoS One* **8**, e61381 (2013).

52. Detry, B. et al. Sunitinib inhibits inflammatory corneal lymphangiogenesis. *Investigative ophthalmology & visual science* **54**, 3082-93 (2013).

53. Ambati, J. et al. An animal model of age-related macular degeneration in senescent Ccl-2- or Ccr-2-deficient mice. *Nature medicine* **9**, 1390-7 (2003).

54. Du, H. et al. JNK inhibition reduces apoptosis and neovascularization in a murine model of age-related macular degeneration. *Proceedings of the National Academy of Sciences of the United States of America* **110**, 2377-82 (2013).

55. Zhang, A.H., Sun, H., Qiu, S. & Wang, X.J. Metabolomics in noninvasive breast cancer. *Clinica chimica acta; international journal of clinical chemistry* **424C**, 3-7 (2013).

56. Zhang, X. et al. Metabolic signatures of esophageal cancer: NMR-based metabolomics and UHPLC-based focused metabolomics of blood serum. *Biochimica et biophysica acta* **1832**, 1207-16 (2013).

57. O'Connell, T.M. Recent advances in metabolomics in oncology. *Bioanalysis* **4**, 431-51 (2012).

58. Johnson, C.H. & Gonzalez, F.J. Challenges and opportunities of metabolomics. *Journal of cellular physiology* **227**, 2975-81 (2012).

Table 1: Troubleshooting

Step	**Problem**	**Possible reason**	**Solution**
12	Apparition of cataract.	Use of xylazine/ketamine mixture for anesthesia.	Use avertin as anesthetic.
12	Death of mice.	Anesthetic overdose.	Single injection of avertin should be sufficient?
12	Death of mice.	Hypothermia of mice.	Use a warming plate.
16	Pupils are not dilated enough.	Drop of tropicamide has flow down.	Place another drop of tropicamide on the eye and avoid that mouse remove it.
21	LO can't see the eye fundus	The cover glass is not well placed on the eye	Replace correctly the cover glass with the genteal® drop exactly on the eye
24	Bubble does not appear after laser impact.	The laser is not focused precisely on the Bruch's membrane.	It is necessary to visualize the retina and precisely focus the aiming beam on the retina before activating the laser. Defocusing aiming beam could lead to burns that do not rupture Bruch's membrane and fail to yield CNV

24	Bubble does not appear after laser impact.	The power of the laser is too low.	For laser calibration, perform burns in the retina of a "calibration mouse" starting with relatively low power and gradually increasing until the lowest power that reproducibly ruptures Bruch's membrane is identified by the creation of a bubble.
24	MO can't position correctly the eye.	The eye is not deorbited enough.	Change position to protrude correctly the eye of the mouse.
24	Bleeding occurs after laser.	A retinal vessel has been injured by the laser.	Stop the laser induction on this eye. Notice it correctly in the Laboratory notebook. Exclude this eye of your study.
25	The solution is not delivered into the vitreous.	The solution has been delivered inside the lens.	Remove the needle from the eye and try again.
25	Some liquid flows out the eye.	The syringe has been taken out of the eye too early.	Wait for a few seconds before taking out the syringe.
25	Eye infection occurs following intravitreal injection.	You likely forgot to apply the antibiotic ointment.	Apply rapidly antibiotic ointment on the infected eye.
30C	The eye is difficult to maintain during flat mount preparation.	Too much conjunctive tissue has been removed.	Leave some conjunctive tissue close to the limbus to facilitate eye grip during dissection.
29	The neovascular membrane of the flat mounted choroid is cut into two parts.	The neovascular membrane has been cut during dissection.	Turn the sclera upside down and cut between laser impacts to better see the impact and avoid to cut inside them.
30	The neovascular membrane has disappeared during dissection.	The neovascular membrane sticks to the retina.	Prepare freshly PFA for eye fixation. Use PFA 1%.
30C	The flat mounted choroid is closed like a « flower » and some sides of	PFA is not miscible with the Vectashield. You took too much time to place the cover glass.	Remove the coverslip and stretch out gently the sides of the flat mounted choroid with

	the choroid are folded before mounting.		a delicate tissue forceps (supplemental video3)
30C or 31	No impact or a reduced CNV were founded	The laser power is too high.	A major pitfall is the usage of too much power, because it damages surrounding choriocapillaris and reduces or completely prevents CNV
31	No impact is found on eye section.	Impacts were lost during cryostat sectioning.	Don't pass too much slides between observation's slides during cryostat sectioning.
32B, C	No FITC fluorescence is seen.	FITC-dextran has not been injected appropriately.	Revise intravenous injection of FITC-dextran.
32B, C	FITC-dextran labeled vessels outside the neovascular membrane appear on float mounted choroid.	The retina has not be totally discarded and retinal vessels interfere with choroidal vessels.	Resect completely and carefully the retina.
33	The solution becomes cloudy.	The proteins precipitated into the tube.	Centrifuge at 3000 rpm during 5 minutes at +4°C.
33	NMR signals are broad and not well resolved.	Shims are not well setup.	Setup the shims.
33	NMR signals are broad and not well resolved.	The proteins precipitated into the tube.	Centrifuge at 3000 rpm during 5 minutes at +4°C.

Figure 1

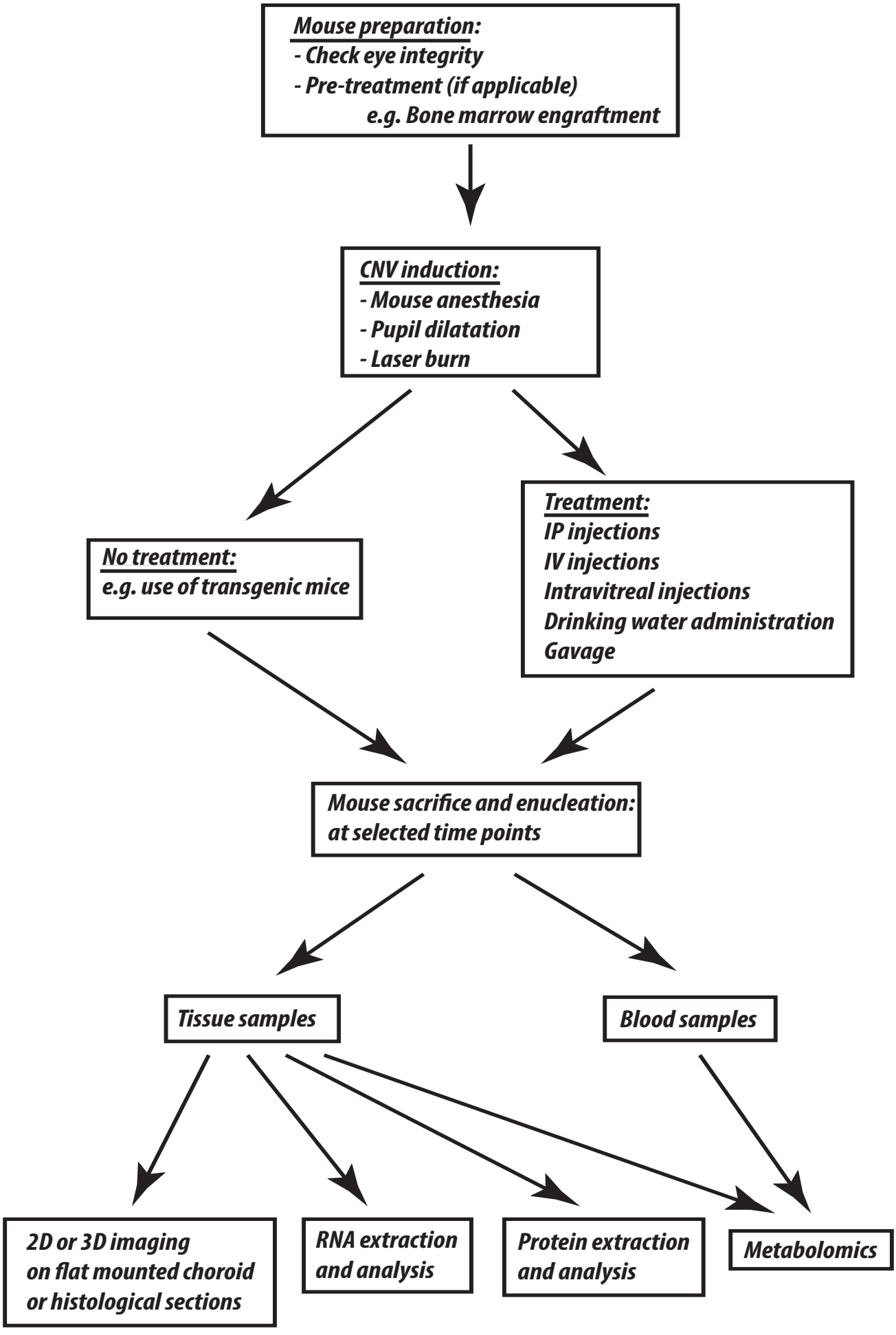
Mouse preparation:
- Check eye integrity
- Pre-treatment (if applicable)
e.g. Bone marrow engraftment
CNV induction:
- Mouse anesthesia
- Pupil dilatation
- Laser burn
No treatment:
e.g. use of transgenic mice
Treatment:
IP injections
IV injections
Intravitreal injections
Drinking water administration
Gavage
Mouse sacrifice and enucleation:
at selected time points
Tissue samples
Blood samples
2D or 3D imaging
on flat mounted choroid
or histological sections
RNA extraction
and analysis
Protein extraction
and analysis
Metabolomics

Figure 2

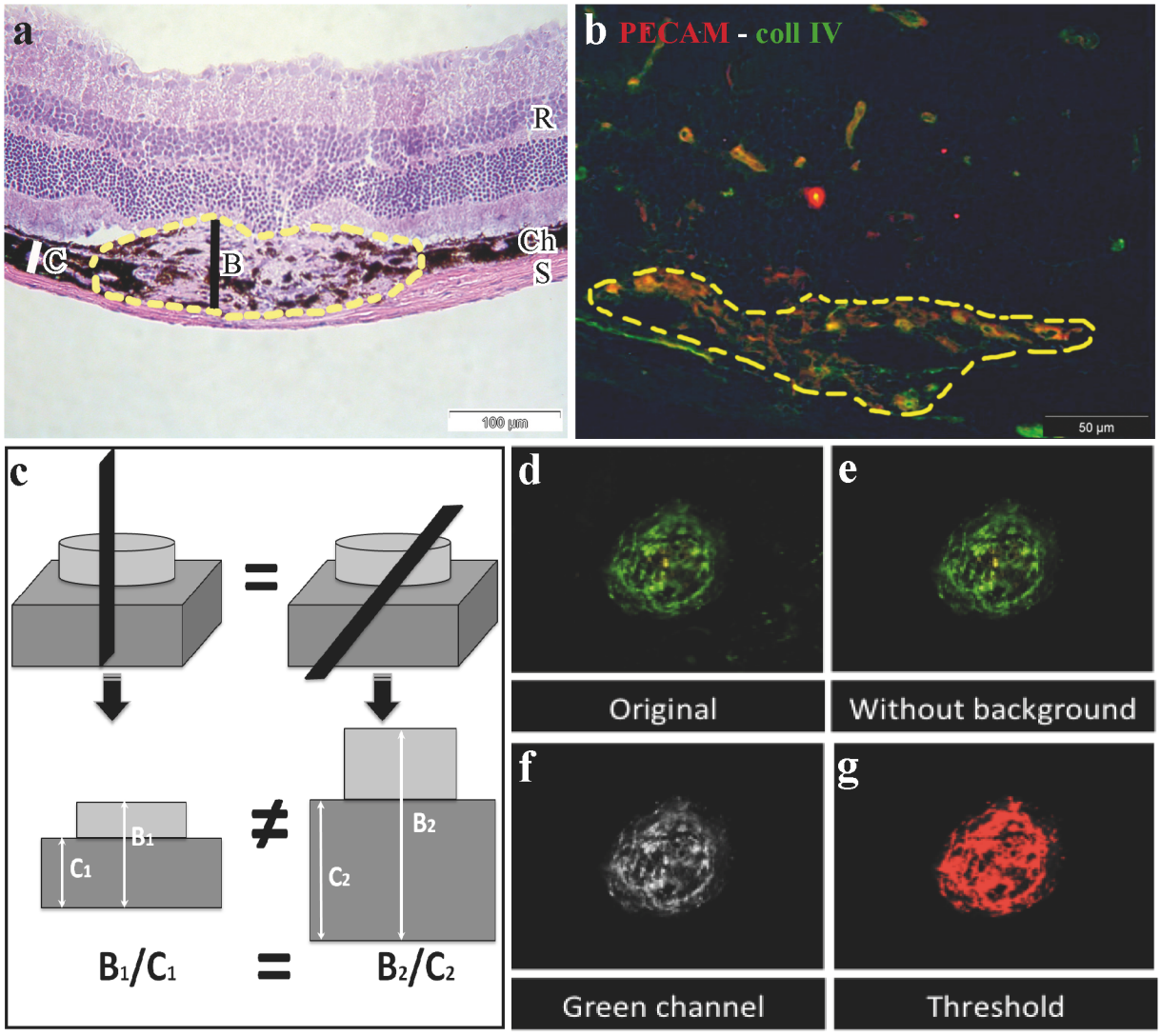
a
R
Ch
S
C
B
100 µm
b PECAM - coll IV
50 µm
c
B1
C1
B2
C2
B1/C1
B2/C2
d
e
Original
Without background
f
g
Green channel
Threshold

Figure 3

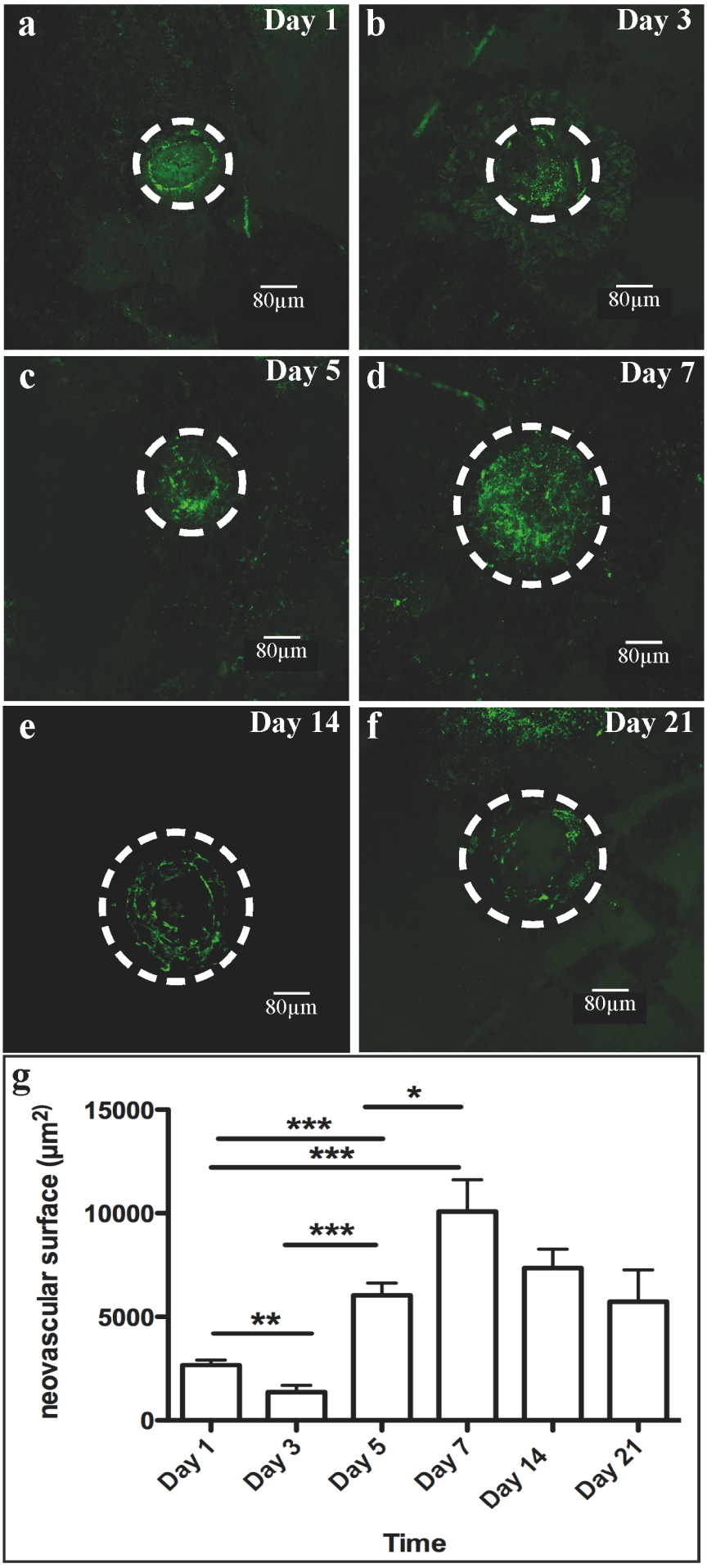
a
Day 1
80µm
b
Day 3
80µm
c
Day 5
80µm
d
Day 7
80µm
e
Day 14
80µm
f
Day 21
80µm
g
neovascular surface (µm²)
15000
10000
5000
0
*
***
***
***
**
Day 1
Day 3
Day 5
Day 7
Day 14
Day 21
Time

Figure 4

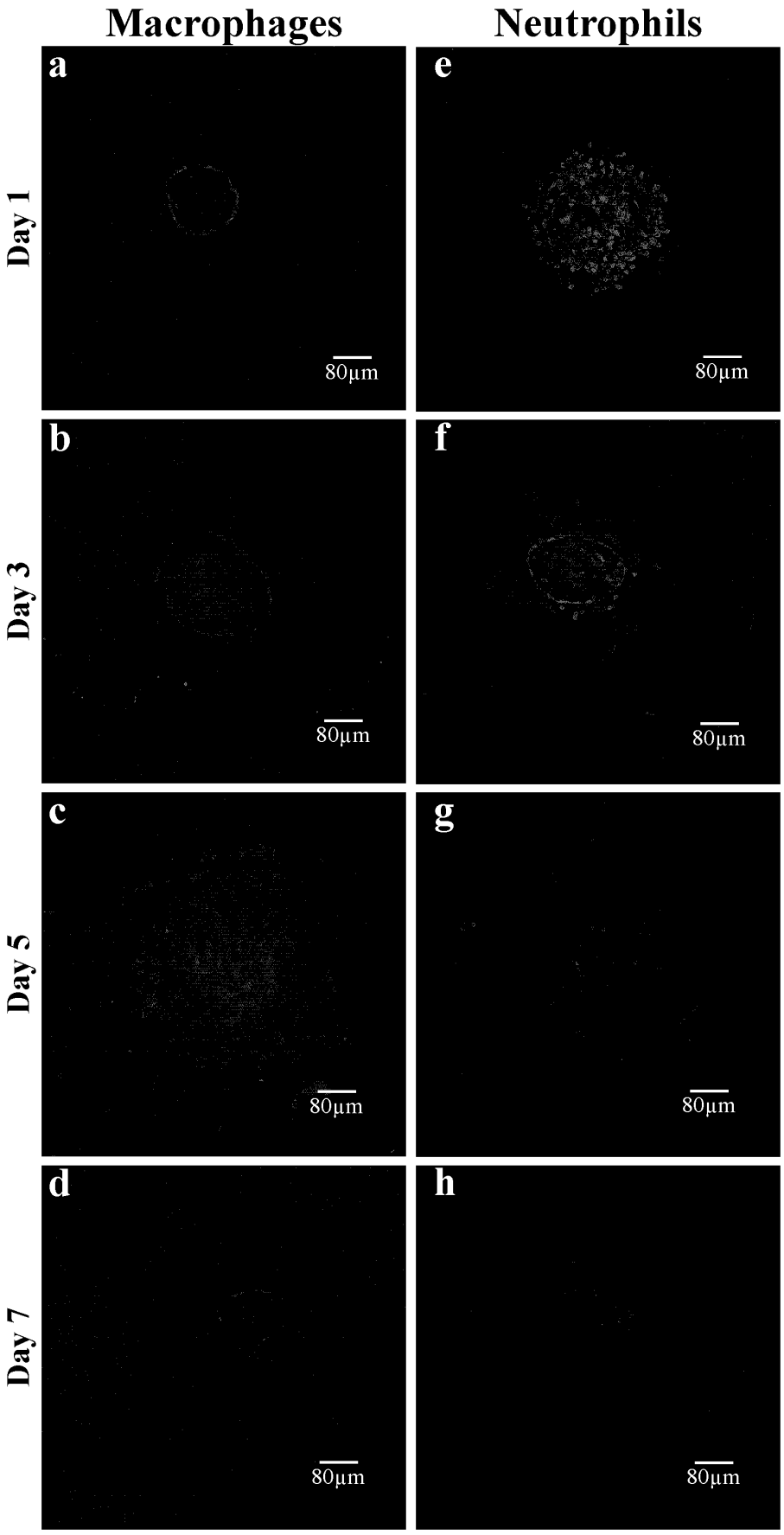
Macrophages
Neutrophils
Day 1
Day 3
Day 5
Day 7
a
b
c
d
e
f
g
h
80μm

Figure 5

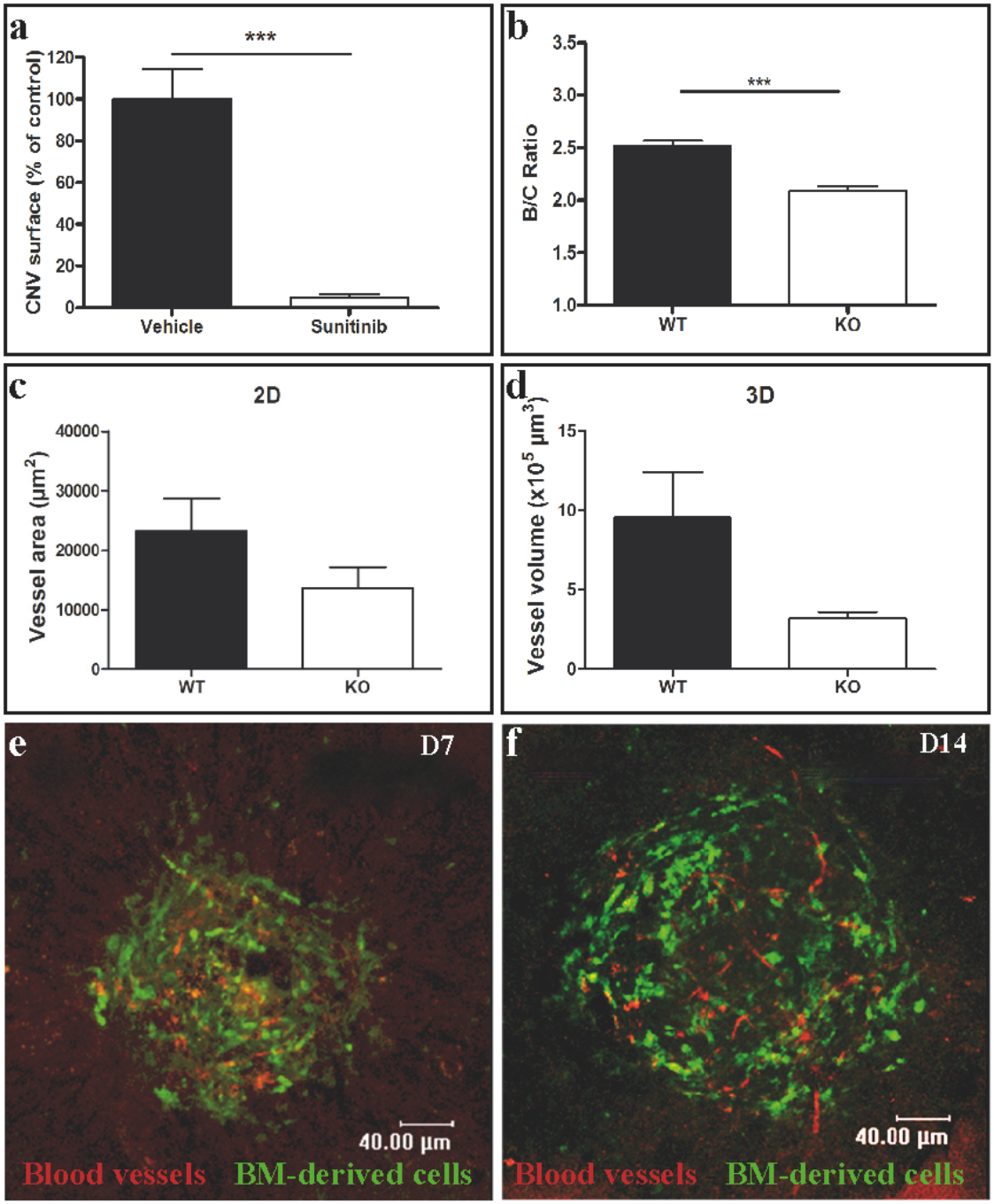
a
***
CNV surface (% of control)
120
100
80
60
40
20
0
Vehicle
Sunitinib
b
***
B/C Ratio
3.5
3.0
2.5
2.0
1.5
1.0
WT
KO
c
2D
Vessel area (µm²)
40000
30000
20000
10000
0
WT
KO
d
3D
Vessel volume (x10⁵ µm³)
15
10
5
0
WT
KO
e
D7
40.00 µm
Blood vessels
BM-derived cells
f
D14
40.00 µm
Blood vessels
BM-derived cells

Figure 6